

# Observation of Negative and Positive Trions in the Electrochemically Carrier-Doped Single-Walled Carbon Nanotubes

Jin Sung Park,<sup>†,‡,¶</sup> Yasuhiko Hirana,<sup>†</sup> Shinichiro Mouri,<sup>‡</sup> Yuhei Miyauchi,<sup>‡,§</sup> Naotoshi Nakashima,<sup>\*,†,||,⊥</sup> and Kazunari Matsuda<sup>\*,‡</sup>

<sup>†</sup>Department of Applied Chemistry, Graduate School of Engineering, Kyushu University, 744 Motooka, Nishi-ku, Fukuoka 819-0395, Japan

<sup>‡</sup>Institute of Advanced Energy, Kyoto University, Uji, Kyoto 611-0011, Japan

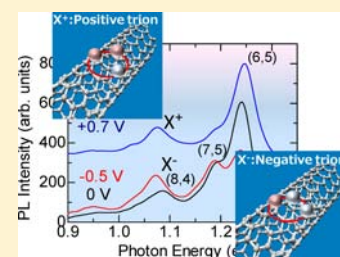
<sup>§</sup>Precursory Research Embryonic Science and Technology (PRESTO), Japan Science and Technology Agency (JST), 4-1-8 Honcho Kawaguchi, Saitama 332-0012, Japan

<sup>||</sup>International Institute for Carbon-Neutral Energy Research (WPI-I2CNER), Kyushu University, 744 Motooka, Nishi-ku, Fukuoka 819-0395, Japan

<sup>⊥</sup>Core Research of Evolutional Science & Technology (CREST), Japan Science and Technology Agency (JST), 5 Sanbancho, Chiyoda-ku, Tokyo 102-0075, Japan

## Supporting Information

**ABSTRACT:** Understanding of electronic and optical features of single-walled carbon nanotubes (SWNTs) has been a central issue in science and nanotechnology of carbon nanotubes. We describe the detection of both the positive trion (positively charged exciton) and negative trion (negatively charged exciton) as a three-particle bound state in the SWNTs at room temperature by an *in situ* photoluminescence spectroelectrochemistry method for an isolated SWNT film cast on an ITO electrode. The electrochemical hole and electron dopings enable us to detect such trions on the SWNTs. The large energy difference between the singlet bright exciton and the negative and positive trions showing a tube diameter dependence is determined by both the exchange splitting energy and the trion binding energy. In contrast to conventional compound semiconductors, on the SWNTs, the negative trion has almost the same binding energy to the positive trion, which is attributed to nearly identical effective masses of the holes and electrons.



## INTRODUCTION

The electronic and optical properties of single-walled carbon nanotubes (SWNTs) have been the subjects of intense investigation because of their importance in nanoscience and for various promising applications.<sup>1</sup> The optically generated electron–hole pair in a 1-nm cylinder structure forms exciton as the strongly bound state, such as the hydrogen atom (H), due to the attractive Coulomb interaction.<sup>2–4</sup> Since the binding energy of an exciton has a high value of  $\sim 200$ – $400$  meV in semiconducting SWNTs<sup>5,6</sup> and of  $\sim 50$  meV even in metallic SWNTs<sup>7</sup> due to the strong quantum confinement in their one-dimensional space, the stable exciton even at room temperature dominates the optical properties of the SWNTs.<sup>8</sup>

Because of the strong Coulomb interaction, the formation of a charged exciton, called a trion, has been expected in carrier-doped SWNTs. The trion is the three-particle bound state of a doped carrier (electron or hole) and an optically generated electron–hole pair, such as  $H^-$  or  $H_2^+$ .<sup>9</sup> Since the trion has an extra charge and nonzero spin, the trion physics has been of strong interest especially in the field of spin manipulation, and has been studied in various semiconducting materials and systems like quantum wells and quantum dots.<sup>10–12</sup> Very recently, the positive trion (bound state of two holes and one

electron) was detected in the hole-doped SWNTs by chemical doping at room temperature.<sup>13</sup> The experimentally estimated binding energy of the positive trion at several tens of meV<sup>13,14</sup> almost agrees with the theoretically calculated one.<sup>15–18</sup> The negative trion (bound state of two electrons and a hole) has also been expected to be stable in the electron-doped SWNTs according to the theoretical prediction.<sup>15–18</sup> However, the negative trion in the SWNTs has not yet been observed by means of chemical doping using a dopant molecule (*n*-dopant). This might be due to the fact that most of the well-known *n*-dopants for SWNTs are unstable in nature and it is difficult to realize a higher electron doping.<sup>19</sup> One of the possible alternatives is an electrochemical technique for the electron or hole doping.<sup>20–28</sup> On the basis of an electrochemical procedure, one can readily donate electrons or holes by changing the Fermi energy of the materials. Hence, the electrochemistry combined with optical spectroscopy is a powerful tool for detecting the negative trion as well as the positive trion.

Received: May 3, 2012

Published: August 7, 2012

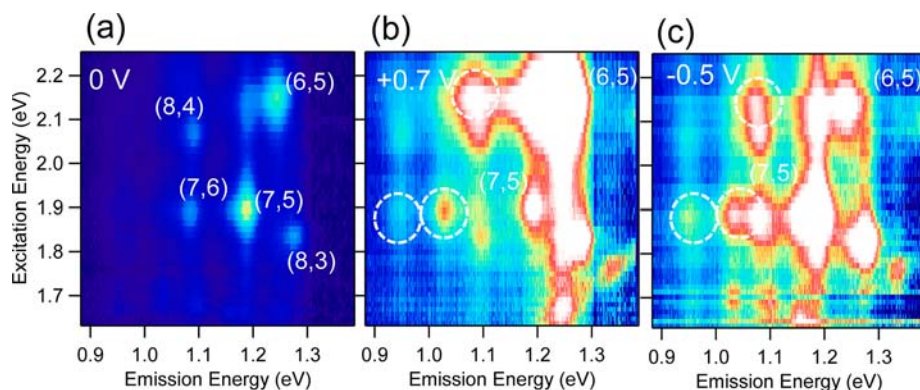


**Figure 1.** PL mapping of the film of the SWNTs on the ITO electrode at the electrochemical potentials of (a) 0 V, (b) +0.7 V, and (c) –0.5 V. The white-dashed circles indicate the new peaks that appeared after electron or hole doping. The peaks that appear at the excitation/emission energy (eV) = 1.33/1.75, 1.02/1.70, 1.1/1.7, and 1.18/1.68 are the exciton peaks from the (9,1)-, (8,6)-, (9,4)-, and (10,2)SWNTs, respectively.

We here demonstrate, for the first time, the optoelectrochemical generation and direct observation of negative trions as well as positive trions on the SWNTs. Moreover, we found that the electrochemically measured negative trions on the SWNTs have almost the same binding energy as the positive trions, which is attributed to nearly identical effective masses of the holes and electrons on the SWNTs.

## EXPERIMENTAL SECTION

**Materials and Sample Preparation of a Film Containing SWNTs on an Electrode.** CoMoCAT-SWNTs (CG-100) were purchased from Southwest NanoTechnologies. For the *in situ* electrochemistry combined with optical spectroscopy (hereafter, *in situ* spectroelectrochemistry), a SWNT sample was added to a D<sub>2</sub>O solution containing 0.1 wt % carboxymethylcellulose sodium salt (Na-CMC, Kishida Chemical), then the mixture was sonicated (Ultrasonic cleaner, Branson 5510) for 2 h followed by centrifugation at 150 000g (Hitachi Himac CS 100GXL) for 10 h in order to exclude as many residual bundles as possible. A hundred microliters aliquot of the supernatant was dropped on a cleaned indium tin oxide (ITO)-coated quartz electrode and then heated at ca. 100 °C to obtain a SWNT/Na-CMC-modified ITO electrode. For the durability of the SWNT/Na-CMC film on the electrode during the electrochemical charging and *in situ* photoluminescence (PL) measurements, an aqueous poly-(diallyldimethylammonium chloride) (PDDA, 20 wt %, Aldrich) solution (50 μL) was dropped on the film, and rinsed with distilled water to remove the excess PDDA to obtain a film of SWNT/Na-CMC/PDDA on the electrode, in which the Na-CMC and PDDA form a poly ion complex that is not soluble in the aqueous solution.<sup>27,28</sup>

**Measurements.** Atomic force microscopic image was measured using an Agilent Technologies 5500 scanning probe microscope for the SWNTs embedded in a CMC film on mica.

All the spectroelectrochemistry measurements in this study were performed using the conventional three-electrode system, which consists of an Ag/AgCl (saturated KCl) reference electrode, a Pt wire counter electrode, and the modified ITO working electrode under an Ar gas atmosphere.<sup>27,28</sup> The electrolyte solution is 0.3 M aqueous NaCl containing 30 mM Na<sub>2</sub>HPO<sub>4</sub> (pH 8). For the *in situ* PL and near IR absorption spectroelectrochemistry, we used a spectrofluorometer (HORIBA JOBIN YVON, FL3-21) and spectrophotometer (JASCO, V-570), respectively, both of which were equipped with a potentiostat (TOHO Technical Research Co., PS-06). The SWNT/CMC-Na/PDDA-modified ITO working electrode was vertically inserted in a quartz cell, which has a light-path length of 10 mm. The cell was filled with the electrolyte solution, in which the reference and counter electrodes were placed so as not to interrupt the light path.

## RESULTS AND DISCUSSION

We measured an AFM image of the SWNTs embedded in the films, and found that many SWNTs are individually dispersed in the film since the height of the tubes is smaller than 2 nm (see Supporting Information, Figure S1).

We first carried out *in situ* vis-near IR absorption spectroelectrochemistry of a SWNT film on the electrode (see Supporting Information, Figure S2);<sup>27,28</sup> however, the detection of trions of the SWNTs was difficult because the near-IR absorption peaks from the SWNTs with several different chirality indices have similar band gaps that overlap one another. Then, we used *in situ* vis-near IR PL spectroelectrochemistry toward the goal. A clear PL response from the SWNTs/CMC-Na/PDDA film on the ITO electrode was detected (see Supporting Information, Figure S3). In this study, the CG100-CoMoCAT SWNTs were used so that we could detect PL signals from the five different (*n,m*)SWNTs. The negative- and positive-potentials were applied to the film on the ITO electrode for donation of the electron and hole to the SWNTs, respectively. Figure 1 shows the PL excitation mapping before and after the electrochemical doping on the SWNT film at room temperature. As shown in Figure 1a, the PL mapping before the doping (0 V) shows the signals of the *E*<sub>11</sub> singlet bright excitons from mainly only five chiral indices of the SWNTs including (8,3), (7,5), (7,6), (8,4) and (6,5). In particular, the (7,5) and (6,5)SWNTs show predominant PL intensities as seen in Figure 1a. We mainly focus on the change in the PL spectra for these SWNTs.

First, we applied the potential of +0.7 V to the SWNT film for the hole doping (for details about the electrochemistry of the SWNTs embedded in a film on an electrode, see Supporting Information, page S2). As shown in Figure 1b, new peaks are observed below the emission energies of the *E*<sub>11</sub> bright exciton peaks of the (6,5), (7,5), and (7,6)SWNTs as marked by the white-dashed circles. When we apply a positive potential, the Fermi energy shifts down to the valence band of the SWNTs, which causes the oxidation. Here the oxidation reaction means a hole doping process on the SWNT. The excitation energies of the new peaks correspond to those of the *E*<sub>11</sub> bright excitons, and the emission energies of the new PL peaks are in good agreement with the energies of positive trions obtained by chemical doping reported by Matsunaga et al.<sup>13</sup> These experimental facts strongly suggest that the new PL peaks in the hole-doped SWNT film (Figure 1b) arise from the positive trions.

Next, the negative potential of  $-0.5$  V was applied for the electron doping, in which the reduction process occurs and the Fermi energy shifts down to the conduction band side. Here the reduction reaction means an electron doping process to the SWNTs. Figure 1c shows that new peaks are observed below the  $E_{11}$  exciton peaks of the (6,5), (7,5), and (7,6)SWNTs as marked by the white-dashed circles, as well as in the case of the positive electrochemical potential in Figure 1b. The appearances of new peaks are closely related to the applied electrochemical potential. Thus, we expect that a doped electron forms a bound state with an optically generated electron–hole pair in the SWNTs, similar to the positive potential case.

To further investigate the new peaks observed in the PL mapping depending on the electrochemical doping level, we measured the PL spectra by varying the applied electrochemical potential. Panels a and c, of Figure 2 show the PL spectra with

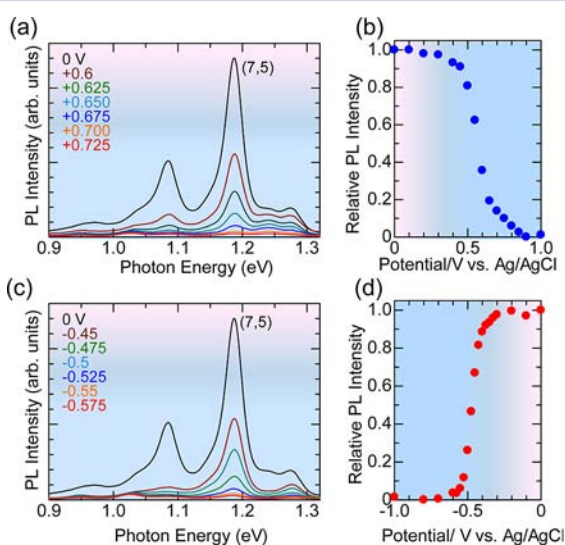


**Figure 2.** PL spectra of the film of the SWNTs on the ITO electrode under (a) positive potential (hole-doped) and (c) negative potential (electron-doped) conditions. The PL intensity change in the exciton peak as a function of the electrochemical potential for the (7,5)SWNTs along (b) the positive direction for the hole doping, and (d) the negative direction for the electron doping.

an excitation energy of  $1.89$  eV for the (7,5) SWNTs as a function of the electrochemical potential on the positive and negative potential sides, respectively. The  $E_{11}$  PL intensity drastically decreases as the electrochemical potential increases in the positive direction for the hole doping, and in the negative direction for the electron doping. These results indicate that the hole (electron) doping occurred in the (7,5)SWNTs by the electrochemical method, because the PL intensity of the  $E_{11}$  exciton decreases due to the state filling of the valence (or conduction) band by the doped carriers, and/or the increase in the doping-induced nonradiative decay rate.<sup>29,30</sup> These effects depend on the doped-carrier density. The decrease in the PL intensity of the  $E_{11}$  exciton by the electrochemical doping is similar to that by the doping of molecules with a high electron-affinity such as  $F_4TCNQ$ .<sup>30</sup> Panels b and d of Figure 2 show the PL intensities of the  $E_{11}$  exciton in the (7,5)SWNTs as a function of the electrochemical potential on the positive and negative potential sides, respectively. The  $E_{11}$  PL intensity was found to drastically decrease around  $+0.55$  and  $-0.45$  V as the

electrochemical potential increased to the positive direction for the hole doping, and to the negative direction for the electron doping, respectively. The asymmetric behavior of the peak intensity for the positive and negative potential is described in the Supporting Information (page S3).

On the basis of the results in Figure 2b,d, the oxidation potential  $E_{ox}$  (reduction potential  $E_{red}$ ) corresponding to the first valence band  $v_1$  (the first conduction band  $c_1$ ) from the Fermi level can be estimated from the positive electrochemical potential voltage (negative electrochemical potential voltage), in which the PL intensity drastically decreases. The sum of the  $E_{red}$  and  $E_{ox}$  corresponding to the energy gap of the SWNTs is consistent with the previously reported value ( $\sim 1.18$  eV).<sup>27,28</sup> It should be noted that much higher electron (or hole) doping can be realized in the electrochemical method than in the chemical doping method using redox molecules from the behavior of the completely suppressed PL intensity (for electric field effect on the electrochemical experiments, see Supporting Information, page S2).

We then focused on the change in the new peak below the  $E_{11}$  exciton peak of the (7,5)SWNTs in the positive potential range from  $+0.60$  to  $+0.75$  V. The result is shown in Figure 3a

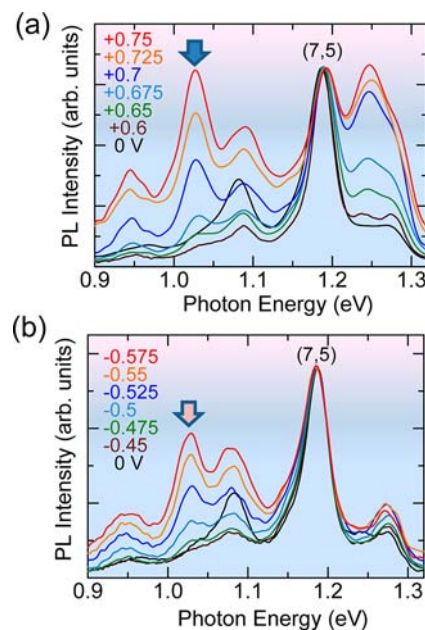


**Figure 3.** Normalized PL spectra of the film of the SWNTs on the ITO electrode under (a) positive potential (hole-doped) and (b) negative potential (electron-doped) conditions.

in which the PL spectra were normalized by the  $E_{11}$  exciton peak intensity of the (7,5)SWNTs. The relative intensities of the newly appeared peaks (marked by arrow) drastically increased as the positive electrochemical potential depending on the hole-doping level increased above  $+0.60$  V, while no new peaks were visible below  $+0.60$  V. The energy positions of the new PL peaks and the quenching behavior of the PL intensity by the electrochemical hole-doping are consistent with those of the positive trion studied by the chemical hole-doping using  $F_4TCNQ$ ,<sup>13</sup> indicating that the new PL peaks, which appeared by the electrochemical hole-doping, arise from the positive trions (positively charged excitons) in the hole-doped SWNTs.

Figure 3b shows the change in the new PL peak below the  $E_{11}$  exciton peaks in the negative potential range from  $-0.45$  to



−0.575 V. As similar to the behavior in the positive potential range, the relative intensity of the new PL peak of the (7,5)SWNTs drastically increased with the increasing negative electrochemical potential above −0.45 V. The relative PL intensity of the new peak was found to be sensitive to the electron-doping level, and these energy positions were similar to those of the positive trions in the hole-doped SWNTs as discussed below in detail (for the detected new peaks from other different chiralities at positive- and negative electrochemical potential application processes, see Supporting Information, Figures S4–S6). These experimental results strongly indicate that the new PL peaks in the negative potential range arise from the negative trions (negatively charged excitons) in the electron-doped SWNTs. Knowing the PL signals from the trions with both positive and negative charges, we can discuss the energy relationship between the positive and negative trion peaks. Panels a and b of Figure 4

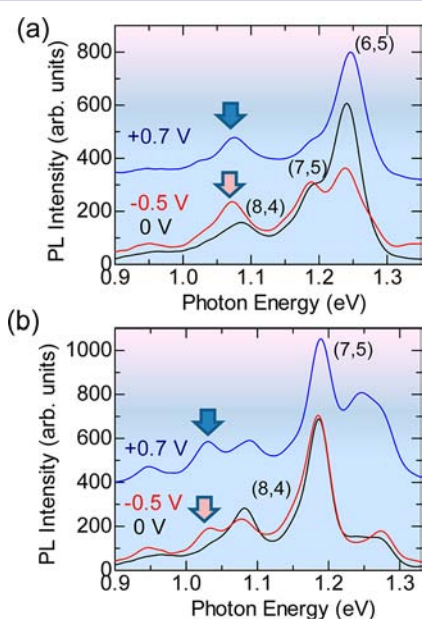


**Figure 4.** PL spectra with the excitation photon energies of (a) 1.89 eV, and (b) 2.16 eV at the electrochemical potential of −0.5 V (red), 0 V (black), and +0.7 V (blue). The three PL spectra were normalized to clearly observe the trion peaks.

show the PL spectra at the nondoped (0 V), hole-doped (+0.7 V) and electron-doped (−0.5 V) conditions with the excitation photon energy of 1.89 and 2.16 eV, respectively. The positive trion peaks (blue arrows) at a hole-doped condition and the negative trion peaks (red arrows) at an electron-doped condition are observed at around 1.07 eV in the (6,5)SWNTs and at 1.03 eV in the (7,5)SWNTs, as shown in Figure 4, panels a and b, respectively. In both cases, the energy positions of the positive and negative trions are very similar to each other. The energy separations,  $\Delta E^+$  ( $\Delta E^-$ ), defined as the difference between the  $E_{11}$  exciton and the positive (negative) trion energy, are very high values of 140–170 meV. The  $\Delta E^+$  is almost consistent with the value in previous results by chemical *p*-doping<sup>13</sup> and strong photo-excitation experiments.<sup>14</sup>

We measured the change in the exciton and trion peak energies as a function of the applied electrochemical potential, and the result is shown in the inset of Figure 5. The estimated  $\Delta E^+$  ( $\Delta E^-$ ) exhibits almost no change with an increase in the

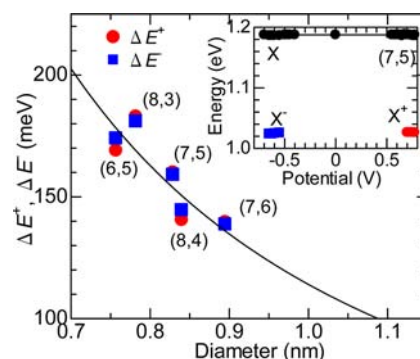


**Figure 5.** Diameter dependence of the  $\Delta E^+$  ( $\Delta E^-$ ). The red circles and blue squares represent the positive and negative trions, respectively. The black line indicates the fitting result by  $\Delta E^+$  ( $\Delta E^-$ ) =  $A/d + B/d^2$ , where  $A$  and  $B$  are  $49 \pm 5$  [meV·nm<sup>2</sup>] and  $65 \pm 5$  [meV·nm], respectively. The inset shows the energy positions of the  $E_{11}$  exciton (X) and positive (negative) trion  $X^+$  ( $X^-$ ) peak as a function of the applied potential.

positive (negative) electrochemical potential. Figure 5 shows the diameter dependence of  $\Delta E^+$  for the positive trion and  $\Delta E^-$  for the negative trion of various chiral indices. Both  $\Delta E^+$  and  $\Delta E^-$  are found to exhibit a clear diameter dependence and some specific patterns due to the family pattern that are well-known electronic characteristics of SWNTs similar to the exciton binding energy.<sup>31</sup> The diameter dependence of the  $\Delta E^+$  and the pattern are quite consistent with those reported in previous results,<sup>13,14</sup> which also indicates that the obtained  $\Delta E^-$  in the electrochemical measurements are due to the negative trions in the electron-doped SWNTs. The extremely high energy separation,  $\Delta E^+$  ( $\Delta E^-$ ), of 140–170 meV is attributed to the trion binding energy and the singlet–triplet exciton splitting. The strong electron–hole exchange interaction originating from the short-range Coulomb interaction increases the singlet exciton energy, while the triplet exciton energy in the SWNTs is constant.<sup>32</sup> Consequently, the exciton states have a high singlet–triplet splitting that has a  $1/d^2$  dependence according to the theoretical results.<sup>32–35</sup> The trion binding energy is defined as the dissociation energy of the triplet exciton and doped carrier (electron or hole). Assuming that the trion binding energy is proportional to the inverse diameter  $1/d$ ,<sup>18</sup> the tube diameter dependence of  $\Delta E^+$  ( $\Delta E^-$ ) can be reproduced as  $\Delta E^+$  ( $\Delta E^-$ ) =  $49/d + 65/d^2$  as shown in Figure 5, in which the coefficients are determined by the fitting procedure and consistent with the theoretical calculations.<sup>18,35</sup> Although there are some variations in  $\Delta E^+$  ( $\Delta E^-$ ) due to the family pattern, the fitted result indicated by the solid curve is in good agreement with the experimental data.

We then discuss the difference between  $\Delta E^+$  and  $\Delta E^-$ . The inset of Figure 5 shows that  $\Delta E^+$  for the positive trions is almost the same with the  $\Delta E^-$  for the negative trions within the accuracy of a few meV, which is on the order of a few % for the  $\Delta E^+$  ( $\Delta E^-$ )  $\sim$  160–170 meV. As discussed above, the  $\Delta E^+$  ( $\Delta E^-$ ) is determined by the singlet–triplet exciton splitting and positive (negative) trion binding energy. The obtained almost identical values of  $\Delta E^+$  and  $\Delta E^-$  indicate that the positive and negative trion binding energies are almost same values. This is in stark contrast to that in the compound semiconductor structures, such as the GaAs system, the positive and negative trions can be observed only at very low temperatures less than 20 K, and  $\Delta E^+$  for the positive trion and  $\Delta E^-$  for the negative

trion have different values of  $\sim 25\%$ ,<sup>11</sup> in which the singlet–triplet exciton splitting is negligibly small and the  $\Delta E^-$  ( $\Delta E^+$ ) is dominated by the positive (negative) trion binding energy. The trion binding energy due to the Coulomb interaction strongly depends on the effective mass of the doped carrier (electron or hole). The effective hole mass  $m_h$  for the SWNTs, however, is slightly larger than the effective electron mass  $m_e$ , and the mass ratio  $m_h/m_e$  is  $\sim 1.06$  for a 1-nm diameter tube, which was obtained by the tight binding calculation.<sup>36</sup> Rønnow et al. calculated the positive and negative trion binding energies of the SWNTs as a function of the mass ratio,  $m_h/m_e$ .<sup>17</sup> These calculated results suggested that the positive trion binding energy is only slightly higher than the negative one, but the difference in the positive and negative trion binding energies is expected to be less than a few meV for the mass ratio  $m_h/m_e = \sim 1.06$ . Our experimental finding, that is, the positive and negative trion binding energies are almost the same within the accuracy of a few meV, is quite consistent with the theoretically calculated results.<sup>17</sup> This strongly supports the fact that this is the first observation of negative triions in SWNTs at room temperature by taking advantage of the electrochemical doping method.

## CONCLUSIONS

In this paper, we described a very fundamental SWNT optical feature, that is, the finding of both negatively and positively charged excitons (negative and positive triions, respectively) in the SWNTs; namely, the presented *in situ* PL-spectroelectrochemical doping method successfully creates both the negative and positive triions by controlling the applied electrochemical potential to the electrode in the negative and positive directions, respectively. We have revealed that the binding energy of the negative triions is almost the same as that of the positive triions. This result is due to almost identical effective mass between the electrons and holes in the SWNTs. The observation of both negative and positive triions strongly ensures the existence of triions in the carrier doped-SWNTs, and will allow progress toward spin manipulation in the SWNTs.

## ASSOCIATED CONTENT

### Supporting Information

Detailed description about electrochemical communication between the SWNTs and the electrode, electric field effect on the electrochemical experiments and asymmetric behavior of the PL peaks, AFM image of the SWNTs on a film, 3D-surface PL plot and the electrochemical vis-near IR absorption and PL spectra with changing the applied potential. This material is available free of charge via the Internet at <http://pubs.acs.org>.

## AUTHOR INFORMATION

### Corresponding Author

matsuda@scl.kyoto-u.ac.jp; nakashima-tcm@mail.cstm.kyushu-u.ac.jp

### Present Address

#R&D Center, Samsung Techwin, Seongnam 463-400, Korea.

### Notes

The authors declare no competing financial interest.

## ACKNOWLEDGMENTS

This work was supported by Grants-in-Aid for Scientific Research (No. 22740195 for S.M, No. 21350110 for N.N, No.

22016007 and No. 23340085 for K.M), PRESTO from JST for Y.M, CREST from JST for N.N, Nanotechnology Network Project (Kyushu-area Nanotechnology Network), and Global COE Program (Science for Future Molecular Systems) from the Ministry of Education, Culture, Sports, Science and Technology, Japan.

## REFERENCES

- (1) Jorio, A.; Dresselhaus, G.; Dresselhaus, M. S. *Carbon Nanotubes: Advanced Topics in the Synthesis, Structure, Properties, and Applications*; Springer: Berlin, 2008.
- (2) Ando, T. *J. Phys. Soc. Jpn.* **1997**, *66*, 1066–1073.
- (3) Spataru, C. D.; Ismail-Beigi, S.; Capaz, R. B.; Louie, S. G. *Phys. Rev. Lett.* **2005**, *95*, 247402.
- (4) Perebeinos, V.; Tersoff, J.; Avouris, P. *Nano Lett.* **2005**, *5*, 2495–2499.
- (5) Wang, F.; Dukovic, G.; Brus, L. E.; Heinz, T. F. *Science* **2005**, *308*, 838–841.
- (6) Maultzsch, J.; Pomraenke, R.; Reich, S.; Chang, E.; Prezzi, D.; Ruini, A.; Molinari, E.; Strano, M. S.; Thomsen, C.; Lienau, C. *Phys. Rev. B* **2005**, *72*, 241402.
- (7) Wang, F.; Cho, D. J.; Kessler, B.; Deslippe, J.; Schuck, P. J.; Louie, S. G.; Zettl, A.; Heinz, T. F.; Shen, Y. R. *Phys. Rev. Lett.* **2007**, *99*, 227401.
- (8) Dresselhaus, M. S.; Dresselhaus, G.; Saito, R.; Jorio, A. *Annu. Rev. Phys. Chem.* **2007**, *58*, 719–747.
- (9) Lampert, M. A. *Phys. Rev. Lett.* **1958**, *1*, 450–453.
- (10) Kheng, K.; Cox, R. T.; Daubigne, Y. M.; Bassani, F.; Saminadayar, K.; Tatarenko, S. *Phys. Rev. Lett.* **1993**, *71*, 1752–1755.
- (11) Bracker, A. S.; Stinaff, E. A.; Gammon, D.; Ware, M. E.; Tischler, J. G.; Park, D.; Gershoni, D.; Filinov, A. V.; Bonitz, M.; Peeters, F. M.; Riva, C. *Phys. Rev. B* **2005**, *72*, 035332.
- (12) Teran, F. J.; Eaves, L.; Mansouri, L.; Buhmann, H.; Maude, D. K.; Potemski, M.; Henini, M.; Hill, G. *Phys. Rev. B* **2005**, *71*, 161309.
- (13) Matsunaga, R.; Matsuda, K.; Kanemitsu, Y. *Phys. Rev. Lett.* **2011**, *106*, 037404.
- (14) Santos, S. M.; Yuma, B.; Berciaud, S.; Shaver, J.; Gallart, M.; Gilliot, P.; Cognet, L.; Lounis, B. *Phys. Rev. Lett.* **2011**, *107*, 187401.
- (15) Rønnow, T. F.; Pedersen, T. G.; Cornean, H. D. *Phys. Lett. A* **2009**, *373*, 1478–1481.
- (16) Rønnow, T. F.; Pedersen, T. G.; Cornean, H. D. *Phys. Rev. B* **2010**, *81*, 205446.
- (17) Rønnow, T. F.; Pedersen, T. G.; Partoens, B.; Berthelsen, K. K. *Phys. Rev. B* **2011**, *84*, 035316.
- (18) Watanabe, K.; Asano, K. *Phys. Rev. B* **2012**, *85*, 035416.
- (19) Kim, S. M.; Jang, J. H.; Kim, K. K.; Park, H. K.; Bae, J. J.; Yu, W. J.; Lee, T. H.; Kim, G.; Loc, D. D.; Kim, U. J.; Lee, E.-H.; Shin, H.-J.; Choi, J.-Y.; Lee, Y. H. *J. Am. Chem. Soc.* **2009**, *131*, 327–331.
- (20) Kavan, L.; Rapta, P.; Dunsch, L. *Chem. Phys. Lett.* **2000**, *328*, 363–368.
- (21) Kavan, L.; Rapta, P.; Dunsch, L.; Bronikowski, M. J.; Willis, P.; Smalley, R. E. *J. Phys. Chem. B* **2001**, *105*, 10764–10771.
- (22) Kazaoui, S.; Minami, N.; Matsuda, N.; Kataura, H.; Achiba, Y. *Appl. Phys. Lett.* **2001**, *78*, 3433–3435.
- (23) Okazaki, K.; Nakato, Y.; Murakoshi, K. *Phys. Rev. B* **2003**, *68*, 035434.
- (24) Corio, P.; Jorio, A.; Demir, N.; Dresselhaus, M. S. *Chem. Phys. Lett.* **2004**, *392*, 396–402.
- (25) Paolucci, D.; Franco, M. M.; Iurlo, M.; Marcaccio, M.; Prato, M.; Zerbetto, F.; Penicaud, A.; Paolucci, F. *J. Am. Chem. Soc.* **2008**, *130*, 7393–7399.
- (26) Ehli, C.; Oelsner, C.; Guldi, D. M.; Mateo-Alonso, A.; Prato, M.; Schmidt, C.; Backes, C.; Hauke, F.; Hirsch, A. *Nat. Chem.* **2009**, *1*, 243–249.
- (27) Tanaka, Y.; Hirana, Y.; Niidome, Y.; Kato, K.; Saito, S.; Nakashima, N. *Angew. Chem., Int. Ed.* **2009**, *48*, 7655–7659.
- (28) Hirana, Y.; Tanaka, Y.; Niidome, Y.; Nakashima, N. *J. Am. Chem. Soc.* **2010**, *132*, 13072–13077.

- (29) Dukovic, G.; White, B. E.; Zhou, Z.; Wang, F.; Jockusch, S.; Steigerwald, M. L.; Heinz, T. F.; Friesner, R. A.; Turro, J.; Brus, L. E. *J. Am. Chem. Soc.* **2004**, *126*, 15269–15276.
- (30) Matsuda, K.; Miyauchi, Y.; Sakashita, T.; Kanemitsu, Y. *Phys. Rev. B* **2010**, *81*, 033409.
- (31) Capaz, R. B.; Spataru, C. D.; Ismail-Beigi, S.; Louie, S. G. *Phys. Rev. B* **2006**, *74*, 121401(R).
- (32) Ando, T. *J. Phys. Soc. Jpn.* **2006**, *75*, 024707.
- (33) Harutyunyan, H.; Gokus, T.; Green, A. A.; Hersam, M. C.; Allegrini, M.; Hartschuh, A. *Nano Lett.* **2009**, *9*, 2010–2014.
- (34) Matsunaga, R.; Matsuda, K.; Kanemitsu, Y. *Phys. Rev. B* **2010**, *81*, 033401.
- (35) Capaz, R. B.; Spataru, C. D.; Ismail-Beigi, S.; Louie, S. G. *Phys. Status Solidi B* **2007**, *244*, 4016–4020.
- (36) Sato, K.; Saito, R.; Jiang, J.; Dresselhaus, G.; Dresselhaus, M. S. *Phys. Rev. B* **2007**, *76*, 195446.